Approaching Fundamental Limits on Bandwidth-to-Thickness Ratio for Electrically Thin Absorbers through Dispersion Engineering

Pardha Sourya Nayani *, Morteza Moradi*, and Younes Radi*,
*Department of Electrical Engineering and Computer Science, Syracuse University, Syracuse, NY 13244, e-mail: yradi@syr.edu

***Abstract*—In numerous applications from radio to optical frequencies including stealth and energy harvesting, there is a need to design electrically thin layers capable of perfectly absorbing electromagnetic waves. From a practical point of view, there is an ever-growing demand for thinner absorbing layers that provide higher absorption bandwidths. However, a theoretical upper limit exists for the bandwidth-to-thickness ratio of passive, linear time-invariant (LTI) metal-backed absorbing layers. Absorbers developed to date, irrespective of their operational frequency range or material thickness, significantly underperform when compared to the upper theoretical limit, failing to exploit the full potential that these LTI metal-backed systems can provide. Here, we introduce a new concept for designing passive ultrathin metal-backed absorbers that can enable absorbing layers with the highest bandwidth-to-thickness ratio ever reported in the literature and can be several-fold higher compared to the same thickness absorbers designed based on conventional approaches. Absorbers designed based on this concept can provide bandwidth-to-thickness ratio arbitrarily close to the fundamental theoretical limit for passive, LTI metal-backed structures. Using the proposed concept, we have designed and experimentally validated an absorber that demonstrates excellent agreement with the theoretical framework presented.**

***Index Terms*—bandwidth-to-thickness ratio, dispersion engineering, non-Foster, upper bounds.**

I. Introduction

The rapid development of new generations of defense, telecommunication technologies, and energy harvesting systems imposes many technological challenges such as demanding the integration of electromagnetic absorbers in more compact spaces. From a practical point of view, there is an ever-growing demand for thinner absorbing layers that provide higher absorption bandwidths. Two main classical types of electromagnetic absorbers include Dallenbach [1] and Salisbury [2] absorbers. Although capable of outstanding absorption at a designated frequency, the inherent requirement of thick layers and the resulting narrow bandwidth limit the applicability of these conventional absorbers in many applications. In recent years, employing artificially engineered surfaces, such as high-impedance surfaces (HIS) and metasurfaces, has revitalized the field of ultrathin absorbers, providing a considerable improvement in design flexibility and miniaturization [3]–[5]. Despite achieving significantly reduced thicknesses compared to their traditional counterparts, these ultrathin absorbers often suffer from limitations in bandwidth. From a practical perspective, a key objective has been to engineer absorbers with minimal thickness while reducing reflectance across the widest possible bandwidth. Nonetheless, Rozanov's investigation established the fundamental limit on the maximum absorption bandwidth-to-thickness ratio for thin, metal-backed slab absorbers which is expressed as :

$$\frac{\Delta\lambda}{d} = \frac{2\pi^2\mu_s}{|ln\,\rho_0|} \tag{1}$$

Here μ_s is the static relative permeability of the slab and ρ_0 is the maximum allowable reflection [6]. Subsequently, a comparable upper bound on the absorption bandwidth-to-thickness ratio for thin absorbers based on artificially engineered surfaces (HIS or metasurfaces) were established [7], [8]. However, to date, absorbers – regardless of their operational frequency range, thickness, and complexity – significantly underperform relative to the fundamental limit defined by Rozanov, failing to exploit the full potential these LTI systems can provide. Here, we introduce a new design methodology for ultrathin absorbers that can enable thin absorbers with bandwidth-to-thickness ratio arbitrarily close to Rozanov's ultimate limit. In the proposed concept, the absorber consists of a passive non-Foster grid meticulously designed based on dispersion engineering. Furthermore, we established a new upper bound on the bandwidth-to-thickness ratio for ultrathin absorbers based on this theory, reaching 95.5% of the fundamental limit established by Rozanov [6]. As proof of principle, we designed and experimentally validated an absorber based on this concept, demonstrating excellent agreement with our predictions.

II. Theory

A. Conventional Absorbers

Consider a generic electrically thin HIS-based absorber (Fig. 1a). Assuming a perfect electric conductor for the ground plane and air as the spacer between the ground plane and the grid, the input admittance of the metal-backed spacer can be approximated as $Y_{md} \approx -j/(\omega\mu_0 d)$. Hence, in our transmission line model, we can readily substitute this thin metal-backed dielectric spacer with an inductor having an inductance value of $L_{md} = \mu_0 d$ as shown in Fig. 1a. Now, for the absorber to be perfectly matched to the free space, the grid should provide the admittance equal to $Y_g^{Req} = 1/\eta_0 + j/(\mu_0\omega d)$ [9].

978-88-31299-10-7/25/$31.00 ©2025 IEEE

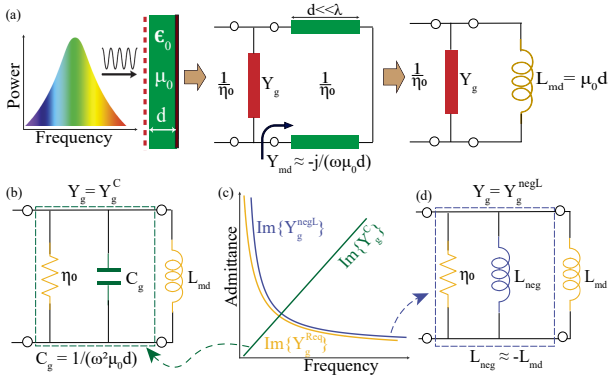

Fig. 1. (a) Illustration of HIS based thin absorbers under normal incidence (b) The conventional way of achieving perfect matching using a capacitive grid. (c) Profiles of the imaginary parts of admittance provided by the capacitive grid ($Im\{Y_g^C\}$), negative inductor grid ($Im\{Y_g^{negL}\}$), and required grid admittance $Im\{Y_g^{Req}\}$. (d) Matching network employing negative inductor.

The conventional way of accomplishing this is by employing a capacitive sheet in parallel with a resistive layer directly above it as shown in Fig. 1b ($Y_g^C = 1/\eta_0 + j\omega C_g$) . However, close examination of the imaginary parts of required grid admittance [i.e., $Im\{Y_g^{Req}\} = 1/(\mu_0 d\omega)$] and the admittance provided by the capacitive grid [i.e., $Im\{Y_g^C\} = \omega C_g$] reveals that, in this scenario, perfect matching can only happen at a single frequency. This is the case because the admittance required for wideband absorption and that provided by the capacitive grid exhibit opposite signs in their slopes, i.e., $\partial[Im\{Y_g^{Req}\}]/\partial\omega = -1/[\mu_0\omega^2 d] < 0$ and $\partial[Im\{Y_g^C\}]/\partial\omega = C_g > 0$ [see Fig. 1c] eliminating the possibility of achieving broadband matching in this scenario. The analysis of $Im\{Y_g^{Req}\}$ indicates that the required admittance corresponds to a negative inductor with inductance $L_{neg} = -\mu_0 d$ (Fig. 1d). This represents a non-Foster element, typically implemented using a power-intensive, complex circuit that often encounters significant challenges related to stability and bandwidth limitations [10]. In the following subsections, we will introduce a new concept based on dispersion engineering, which enables emulating the characteristics of a negative inductor over a desired bandwidth within a fully passive platform.

B. Realizing negative inductors using dispersion engineering

To design passive, time-invariant non-Foster reactive elements, dissipation (loss) must be introduced into the system, which can be accomplished through a platform that enables flexible dispersion engineering. One potential platform to achieve this is by utilizing a parallel-plate capacitor with capacitance C_0 filled with a dielectric that follows Lorentzian dispersion (see Fig. 2a). Similar dispersive platform was used by Yaghjian to nullify the Q energy associated with a matching capacitor in the matching network of electrically small antennas [11]. The admittance for such a capacitor can be expressed as $Y_g^{DisC}(\omega) = j\omega C_0\,[\epsilon(\omega)/\epsilon_0]$, where $\epsilon(\omega)/\epsilon_0$ is the Lorentzian relative permittivity which is given as $\epsilon(\omega)/\epsilon_0 = 1+(\omega_p/\omega_0)^2\,/[1-(\omega/\omega_0)^2+j\,(\gamma/\omega_0)\,(\omega/\omega_0)]$. Here ω_0 represents the resonance frequency, ω_p is the plasma frequency, and γ is the damping constant. To achieve a negative inductor, the imaginary component of $Y_g^{DisC}(\omega)$ must possess a positive value and exhibit a negative slope at the design frequency. A closer investigation of the admittance of this capacitor reveals that at frequencies $\omega >> \omega_0$ and $\omega << \omega_0$, the slope of $Im\{Y_g^{DisC}\}$ will always be positive. However, at the resonance frequency ($\omega = \omega_0$), the situation is different, where $\partial[Im\{Y_g^{DisC}(\omega)\}]/\partial\omega\big|_{\omega=\omega_0} = C_0\left(1 - \frac{2\omega_p^2}{\gamma^2}\right)$ which can be made negative if $\gamma < \sqrt{2}\omega_p$, while the imaginary component of the admittance remains positive $Im\{Y_g^{DisC}(\omega)\} > 0$. Furthermore, $\partial[Re\{Y_g^{DisC}(\omega)\}]/\partial\omega\big|_{\omega=\omega_0} = 0$, indicating that this design not only provides the required non-Foster characteristics but also ensures a flat real part, i.e., dispersionless resistor in parallel to the negative inductor around $\omega = \omega_0$ (see Fig. 2b). However, it is extremely difficult if not impossible, to realize such a capacitor filled with a material with precisely engineered dispersion. In fact, this capacitor can be realized using a simple circuit network composed of frequency-independent elements. Figure. 2c represents one of the many circuit realizations for the capacitor filled with highly dispersive Lorentzian dielectric. Now that we have a platform that can provide a non-Foster negative inductor over a desired bandwidth, we can employ it in designing ultimately thin wideband absorbers.

C. Designing thin wideband absorbers using dispersive grids

In order to achieve maximum absorption bandwidth-to-thickness we derive specific relations for the dispersion parameters of the grid admittance by imposing two critical conditions at the design frequency, ω_0 : $Im\{Y_g^{Req}\} = Im\{Y_g^{DisC}\}$ and reflection magnitude being maximum threshold value (i.e., ρ_0). Imposing these specified conditions results in $C_0 = 1/[\mu_0\omega_0^2 d]$ and $\omega_p = \omega_0\sqrt{\left(\frac{\mu_0 d\gamma}{\eta_0}\right)\left(\frac{1+\rho_0}{1-\rho_0}\right)}$. In this case, the absolute maximum bandwidth $\Delta\omega_{max}$ happens when $\gamma = \frac{\mu_0\omega_0^2 d}{\eta_0}\left(\frac{1+\rho_0}{1-\rho_0}\right)$. Interestingly, even though this relation was achieved through mathematical derivation, ensuring that $Im\{Y_g^{Req}\}$ and $Im\{Y_g^{DisC}\}$ display equal negative slopes around ω_0, i.e., $\partial[Im\{Y_g^{Req}(\omega)\}]/\partial\omega|_{\omega=\omega_0} = \partial[Im\{Y_g^{DisC}(\omega)\}]/\partial\omega\big|_{\omega=\omega_0}$, also leads to the same condition on γ. For this case, the maximum achievable bandwidth-to-thickness ratio can be derived as

$$\frac{\Delta\lambda}{d} = 4\pi\frac{\sqrt{\rho_0}}{1-\rho_0}. \tag{2}$$

To demonstrate this idea, we design an electrically-thin absorber at frequency $f_0 = 10$ GHz and thickness $d = \lambda_0/30$. As shown in the Fig. 2d, the obtained $Im\{Y_g^{DisC}\}$ clearly demonstrates the negative inductive characteristics over a wide frequency band while $Re\{Y_g^{DisC}\}$ exhibits zero slope around ω_0 which is consistent with $Re\{Y_g^{Req}\}$. Fig. 2e further demonstrates the wideband absorption performance achieved by the proposed design.

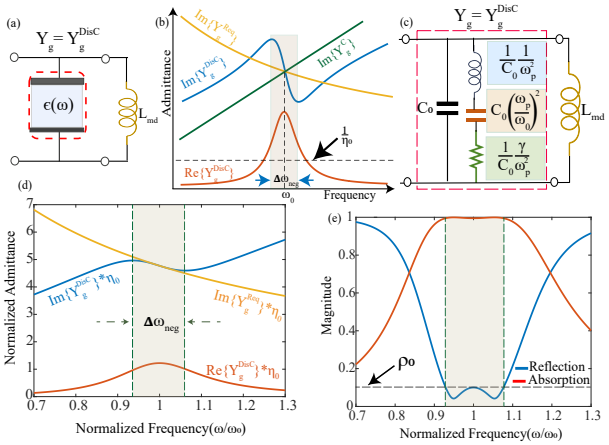

Fig. 2. (a) Matching network using Lorentz dispersive dielectric-filled capacitor (b) Lorentz dispersive dielectric-filled capacitor emulating negative slope around resonant frequency ω_0. (c) One of the many circuit representations of Lorentz dispersive dielectric-filled capacitor. (d) Normalized admittance profiles of dispersion engineered 1^{st} order grid. (e) The reflection and absorption spectrum of a $\lambda_0/30$-thick absorber designed based on theory developed in section II-C with maximum allowable reflection ρ_0 = 0.1.

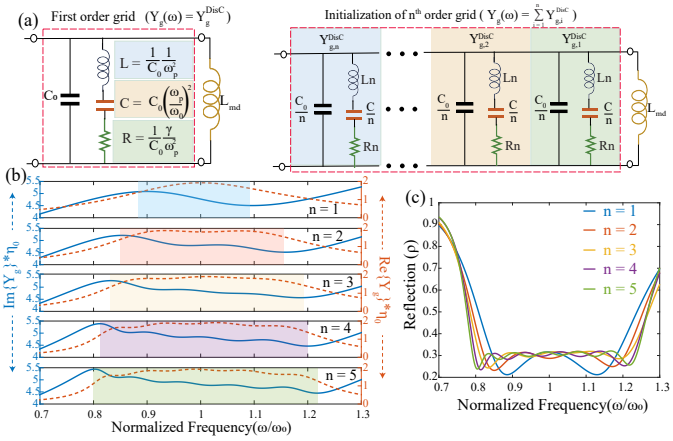

Fig. 3. (a) Initialization of the circuit parameters of higher order grid based on first order design. (b) Admittance profiles for the designed higher order dispersive grid (i.e., $n = 1$ through $n = 5$). (c) The reflection spectrum of the absorber based on higher order dispersive matching.

III. Higher Order Disperive Grid Based Absorbers

This proposed concept can be further enhanced by incorporating higher-order Lorentz dispersion into the platform. Specifically, by adding higher order dispersion into the grid enables achieving a negative slope for the imaginary part and near dispersion-less behavior for the real part of admittance across a broad frequency range, thereby further improving the absorption bandwidth. Building on this, the following subsections will outline a design methodology for absorbers based on higher-order dispersive grids and establish upper bounds on the absorption bandwidth-to-thickness ratio.

A. Design Methodology

Consider a grid characterized by a dispersive dielectric-filled capacitor, where the dielectric's dispersion follows an n^{th}-order Lorentz model. The admittance of this grid can be expressed as follows:$Y_g(\omega) = j\omega \sum_{i=1}^{n} C_{0,i}\left[1 - \frac{\omega_{p,i}^2}{\omega^2 - \omega_{0,i}^2 + j\omega\gamma_i}\right]$ where $C_{0,i}$ is the capacitance of the capacitor with free space between its parallel plates, and $\omega_{p,i}$, $\omega_{0,i}$, γ_i are plasma frequency, resonant frequency, and damping frequency of the i^{th} resonator, respectively. For an n^{th}- order grid the total number of parameters to be determined is $4n$. Determining these design parameters analytically to maximize the achievable bandwidth-to-thickness ratio becomes exceedingly challenging, if not impossible, for orders $n > 1$. To address this, we developed a semi-analytical approach aimed at optimizing the dispersion parameters of a multi-order Lorentz grid to achieve the highest possible absorption bandwidth-to-thickness ratio for a specified allowed reflection. This method closely follows the semi-analytical approach proposed by Rozanov to extract upper bounds on the bandwidth-to-thickness ratio of thin metal-backed dispersive dielectric absorbers with arbitrary orders of dispersion [12] . We begin by considering the first-order design, whose equivalent circuit parameters have been analytically derived for a given thickness d, design frequency f_0, and maximum allowable reflection ρ_0 (see section II-C). The circuit parameters of the multi-order grid are then initialized to provide the same grid admittance as that of the first-order grid, as shown in Fig. 3a. The optimization of these higher-order grid parameters is performed by maximizing the following objective function: $\alpha\left(\frac{\Delta\lambda}{d}\right)^{0.5} - \sum_i (R_i - \rho_0)^2$. Here, R_i represents the i^{th} local maximum of the reflectivity spectrum within the absorption bandwidth, and $\Delta\lambda/d$ denotes the achieved absorption bandwidth-to-thickness ratio. The parameter α acts as a scaling factor to ensure that the first and second terms in the objective function are comparable in magnitude. The purpose of this objective function is to maximize the bandwidth-to-thickness ratio while simultaneously minimizing the penalty associated with the reflection coefficient maxima deviating from ρ_0 within the absorption band. This approach allows for the determination of the optimal design parameters that result in the maximum achievable bandwidth-to-thickness ratio for a given order of dispersion, design frequency, thickness and ρ_0. To demonstrate bandwidth enhancement using higher-order Lorentzian dispersion networks, we designed an electrically thin absorber with dispersion orders ranging from 1 to 5, based on the proposed optimization routine. Fig. 3b clearly shows that as the dispersion order increases, the bandwidth of the negative slope of $Im\{Y_g\}$ expands, and the flatness of $Re\{Y_g\}$ improves. Consequently, Fig. 3c illustrates the corresponding increase in absorption bandwidths with higher dispersion orders.

B. Upper bounds on bandwidth-to-thickness of higher order dispersive grid based absorbers

Based on the proposed optimization routine, we numerically calculated the maximum achievable bandwidth-to-thickness ratio for a given dispersion order n at varying threshold reflectivity ρ_0. By checking the numerical data for second order in Fig. 4a, it turns out that for $\rho_0 \to 0$ and $\rho_0 \to 1$, the data can

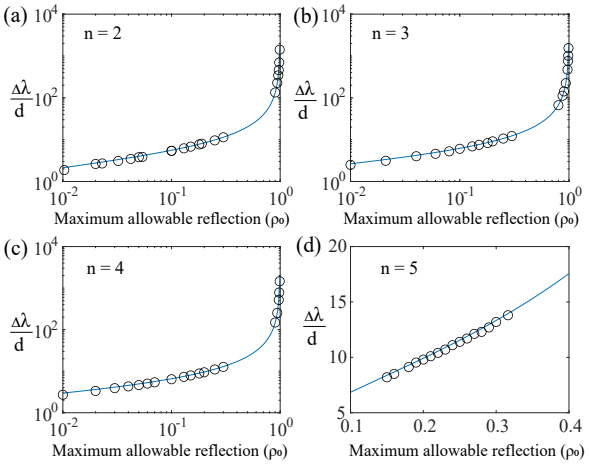

Fig. 4. Maximum achievable $\Delta\lambda/d$ of higher order absorbers. The circles indicate the numerically extracted value and solid lines indicate the determined empirical relation (4) for (a) $n = 2$ (b) $n = 3$ (c) $n = 4$ (d) $n = 5$

be fitted using $\Delta\lambda/d \approx 3\pi\rho_0^{1/3}$ and $\Delta\lambda/d \approx 4.5\pi/(1-\rho_0)$, respectively. By combining these two asymptotic behaviors and considering other reflection data points within this range, we can fit the maximum achievable bandwidth-to-thickness ratio for the 2^{nd} order grid using the following empirical equation:

$$\frac{\Delta\lambda}{d} = 3\pi\frac{\rho_0^{1/3}}{1-\rho_0^{2/3}} \tag{3}$$

Following the similar procedure, the obtained numerical data for $n = 3, 4$ can be fitted using $\frac{\Delta\lambda}{d} = \frac{12}{5}\pi\frac{\rho_0^{1/4}}{1-\rho_0^{1/2}}$ and $\frac{\Delta\lambda}{d} = 2\pi\frac{\rho_0^{1/5}}{1-\rho_0^{2/5}}$, respectively (refer to Fig. 4b and 4c). Through careful analysis of these empirical relations, the maximum achievable bandwidth-to-thickness ratio can be generalized for an arbitrary order of dispersion n as:

$$\frac{\Delta\lambda}{d}(\rho_0, n) = 4\pi\left(\frac{3}{n+2}\right)\frac{\rho_0^{1/(n+1)}}{1-\rho_0^{2/(n+1)}} \tag{4}$$

It is interesting to note that, for $n = 1$, this empirical equation (4), yields the analytical upper bound derived for the first order grid previously, i.e., (2). As a test, Fig. 4d compares the numerically obtained bound for the 5^{th} order with that of the generalized empirical equation when $n = 5$, demonstrating excellent agreement. Subsequently, an ultimate upper limit on bandwidth-to-thickness ratio of dispersive grid-based absorbers is derived when $n \to \infty$ which is expressed as:

$$\lim_{n\to\infty}\frac{\Delta\lambda}{d}(\rho_0, n) = \frac{6\pi}{|ln\,\rho_0|} \tag{5}$$

IV. Results

A. Comparison of bandwidth-to-thickness ratio of proposed concept with existing bounds

Fig. 5a presents a comparison between the absorption bandwidth-to-thickness ratio of the proposed design and established upper bounds in the literature. It is evident that the derived ultimate bound for the dispersive grid-based absorber (5) surpasses all previously established bounds and remarkably achieved 95.5% of the fundamental limit (1) defined by Rozanov. Furthermore, it is fascinating to note that the proposed 4^{th}-order grid exceeds Rozanov's bound for metal-backed dispersive dielectric absorbers with infinite-order dispersion in the dielectric ($\Delta\lambda/d = 48/(\pi|ln\,\rho_0|)$, Eq. 10 in [12], as $n \to \infty$) when $\rho_0 > 0.15$. In contrast, the proposed 5^{th} and higher order grids surpass this bound when $\rho_0 > 0.05$, as illustrated in Figure 5b.

B. Comparison of bandwidth-to-thickness ratio of proposed concept with existing wideband absorbers

So far, we have compared the bandwidth-to-thickness ratio of absorbers designed based on our proposed concept with the fundamental bounds in the literature. However, it is essential to also evaluate the performance of our design against existing wideband absorbers. Fig. 5c and Table. I provides a comparison of the absorption bandwidth-to-thickness ratios of some of the best-performing wideband absorbers across different parts of the frequency spectrum. As demonstrated in this figure, to the best of our knowledge, irrespective of design frequency our first-order design achieves a record high absorption bandwidth-to-thickness ratio. Furthermore, while all other absorbers drastically under perform in exploiting all the potential that these LTI structures can provide, absorbers based on the proposed concept can get arbitrarily close to the fundamental limit.

C. Full wave simulations and measurements

To validate the proposed theory, we designed and measured an absorbing layer incorporating a first-order grid with a thickness of $d = \lambda_0/30$ at a center frequency of 10 GHz and a reflectivity of $\rho_0 = 0.15$. Fig. 5d illustrates the designed unit cell of the admittance grid, while Fig. 5e depicts the measurement setup for the fabricated sample. Fig. 5f compares the measured reflection spectrum of the absorber with simulated and theoretical results, demonstrating strong agreement. The measured response indicates a bandwidth of 1.9 GHz centered at 10 GHz, with reflectivity below -15 dB, very closely aligning with the theoretical predictions. Please note that the propsed design concept is based on the normal wave incidence; however, oblique incidence modifies the matching conditions, resulting in angle-dependent performance. We are currently developing a methodology to achieve wide-angle, wideband thin absorbers.

V. Conclusion

We have developed an innovative design methodology based on dispersion engineering for ultra-thin absorbers, capable of achieving an absorption bandwidth-to-thickness ratio nearing the fundamental limit. Furthermore, we established new upper bounds on this ratio for absorbers composed of dispersive grids, expressed as a function of threshold reflectivity ρ_0 and dispersion order n with the ultimate bound reaching

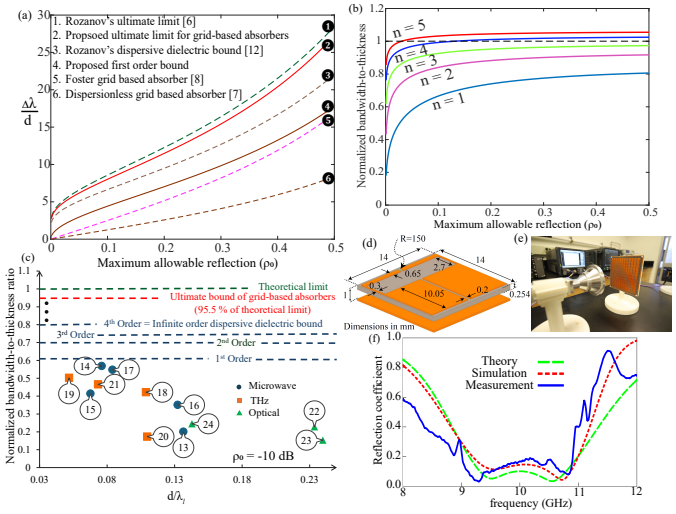

Fig. 5. (a) Comparison of upper bounds on $\Delta\lambda/d$ of the proposed theory with established bounds in literature. (b) Comparison of $\Delta\lambda/d$ of the proposed multi-order order dispersive grid based absorber with Rozanov's upper bound on dispersive dielectric absorber. Please note that y-axis has been normalized with this upper bound. (c) $\Delta\lambda/d$ comparison between the proposed concept, Rozanov's limits, and some of the existing broadband absorbers in literature [13]–[24] . The y axis is reported bandwidth-to-thickness normalized with Rozanov's fundamental limit and x axis is the thickness normalized with wavelength at the lower frequency of absorption band. The numbers on the graph indicate the references. (d) Designed unit cell (e) Experimental setup (f) Simulation and measurement results.

TABLE I
COMPARISON OF WIDEBAND ABSORBERS IN FIG. 5C

Ref	Frequency	Lower Frequency	Higher Frequency	Thickness	Δλ/d
[13]	Microwave	7.80E+09	1.47E+10	$0.14\lambda_l$	3.44
[14]	Microwave	1.90E+09	7.30E+09	$0.076\lambda_l$	9.73
[15]	Microwave	4.23E+09	8.13E+09	$0.07\lambda_l$	7.09
[16]	Microwave	6.30E+09	3.07E+10	$0.13\lambda_l$	6.01
[17]	Microwave	2.70E+09	1.27E+10	$0.08\lambda_l$	9.37
[18]	THz	6.50E+11	3.03E+12	$0.11\lambda_l$	7.22
[19]	THz	6.39E+12	9.47E+12	$0.11\lambda_l$	2.96
[20]	THz	3.34E+13	1.85E+13	$0.05\lambda_l$	8.61
[21]	THz	2.34E+12	5.64E+12	$0.07\lambda_l$	7.98
[22]	Optical	1.80E+15	1.56E+14	$0.23\lambda_l$	3.91
[23]	Optical	4.23E+14	1.15E+15	$0.24\lambda_l$	2.63
[24]	Optical	4.29E+14	1.07E+15	$0.14\lambda_l$	4.20

to 95.5% of the fundamental limit established by Rozanov [6]. Our findings further demonstrate that integrating fourth-order Lorentz dispersion within the impedance grid significantly enhances performance, enabling our design to surpass Rozanov's established limit for metal-backed dielectric absorbers with infinite-order dispersion in dielectric. As proof of principle, we fabricated and experimentally validated our proposed theory using a first-order dispersive grid absorber. The proposed concept enables metal-backed absorbers with the highest bandwidth-to-thickness ratio ever reported in the literature, representing a significant advancement in the design and performance of electromagnetic absorbers.

REFERENCES

[1] W. Dallenbach and W. Kleinsteuber, "Reflection and absorption of decimeter-waves by plane dielectric layers," *Hochfreq. u Elektroak*, vol. 51, pp. 152–156, 1938.

[2] W. W. Salisbury, "Absorbent body for electromagnetic waves," 1952.

[3] B. A. Munk, *Frequency selective surfaces: theory and design*. John Wiley & Sons, 2005.

[4] D. F. Sievenpiper, *High-impedance electromagnetic surfaces*. University of California, Los Angeles, 1999.

[5] C. L. Holloway, E. F. Kuester, J. A. Gordon, J. O'Hara, J. Booth, and D. R. Smith, "An overview of the theory and applications of metasurfaces: The two-dimensional equivalents of metamaterials," *IEEE antennas and propagation magazine*, vol. 54, no. 2, pp. 10–35, 2012.

[6] K. N. Rozanov, "Ultimate thickness to bandwidth ratio of radar absorbers," *IEEE Transactions on Antennas and Propagation*, vol. 48, no. 8, pp. 1230–1234, 2000.

[7] R. Huang, L. B. Kong, and S. Matitsine, "Bandwidth limit of an ultrathin metamaterial screen," *Journal of applied physics*, vol. 106, no. 7, 2009.

[8] Y. Pang, H. Cheng, Y. Zhou, and J. Wang, "Upper bound for the bandwidth of ultrathin absorbers comprising high impedance surfaces," *IEEE Antennas and Wireless Propagation Letters*, vol. 11, pp. 224–227, 2012.

[9] Y. Ra'di, C. R. Simovski, and S. A. Tretyakov, "Thin perfect absorbers for electromagnetic waves: theory, design, and realizations," *Physical Review Applied*, vol. 3, no. 3, p. 037001, 2015.

[10] E. Ugarte-Munoz, S. Hrabar, D. Segovia-Vargas, and A. Kiricenko, "Stability of non-foster reactive elements for use in active metamaterials and antennas," *IEEE transactions on antennas and propagation*, vol. 60, no. 7, pp. 3490–3494, 2012.

[11] A. D. Yaghjian, "Overcoming the chu lower bound on antenna q with highly dispersive lossy material," in *2017 11th European Conference on Antennas and Propagation (EUCAP)*, pp. 1545–1549, 2017.

[12] K. Rozanov and S. Starostenko, "Numerical study of bandwidth of radar absorbers," *The European Physical Journal Applied Physics*, vol. 8, no. 2, pp. 147–151, 1999.

[13] F. Ding, Y. Cui, X. Ge, Y. Jin, and S. He, "Ultra-broadband microwave metamaterial absorber," *Applied physics letters*, vol. 100, no. 10, 2012.

[14] Y. Han and W. Che, "Low-profile broadband absorbers based on capacitive surfaces," *IEEE Antennas and Wireless Propagation Letters*, vol. 16, pp. 74–78, 2016.

[15] M. Saikia and K. V. Srivastava, "Design of thin broadband microwave absorber using combination of capacitive and circuit analog absorbers," in *2018 IEEE Indian Conference on Antennas and Propogation (InCAP)*, pp. 1–4, IEEE, 2018.

[16] Y. Kim, P. Park, J. Jo, J. Lee, L. Jeong, J. Shin, J.-H. Lee, and H.-J. Lee, "Ultrawideband electromagnetic metamaterial absorber utilizing coherent absorptions and surface plasmon polaritons based on double layer carbon metapatterns," *Scientific Reports*, vol. 11, no. 1, p. 23045, 2021.

[17] Y. Zhang, W. Yang, X. Li, and G. Liu, "Design and analysis of a broadband microwave metamaterial absorber," *IEEE Photonics Journal*, vol. 15, no. 3, pp. 1–10, 2023.

[18] G. Varshney, "Wideband thz absorber: by merging the resonance of dielectric cavity and graphite disk resonator," *IEEE Sensors Journal*, vol. 21, no. 2, pp. 1635–1643, 2020.

[19] H.-B. Liu, C.-X. Hu, Z.-L. Wang, H.-F. Zhang, and H.-M. Li, "An ultra-wideband terahertz metamaterial absorber based on the fractal structure," *Plasmonics*, vol. 16, pp. 263–271, 2021.

[20] S. Liang, F. Xu, H. Yang, S. Cheng, W. Yang, Z. Yi, Q. Song, P. Wu, J. Chen, and C. Tang, "Ultra long infrared metamaterial absorber with high absorption and broad band based on nano cross surrounding," *Optics & Laser Technology*, vol. 158, p. 108789, 2023.

[21] G. Wu, X. Jiao, Y. Wang, Z. Zhao, Y. Wang, and J. Liu, "Ultra-wideband tunable metamaterial perfect absorber based on vanadium dioxide," *Optics Express*, vol. 29, no. 2, pp. 2703–2711, 2021.

[22] P. Yu, H. Yang, X. Chen, Z. Yi, W. Yao, J. Chen, Y. Yi, and P. Wu, "Ultra-wideband solar absorber based on refractory titanium metal," *Renewable Energy*, vol. 158, pp. 227–235, 2020.

[23] C. Li, H. Fan, Q. Dai, Z. Wei, S. Lan, and H. Liu, "Multipole resonance in arrays of diamond dielectric: a metamaterial perfect absorber in the visible regime," *Nanomaterials*, vol. 9, no. 9, p. 1222, 2019.

[24] S. Charola, S. K. Patel, K. Dalsaniya, R. Jadeja, T. K. Nguyen, and V. Dhasarathan, "Numerical investigation of wideband l-shaped metasurface based solar absorber for visible and ultraviolet region," *Physica B: Condensed Matter*, vol. 601, p. 412503, 2021.